The Response of Onset and Withdrawal of the Indian Summer Monsoon to Volcanic Aerosols

S. Iyer[1,2], M. Günther[1], C. Jalihal[1,3], and C. Timmreck[1]

[1]Max Planck Institute for Meteorology, Hamburg
[2]Indian Institute of Science Education and Research, Pune
[3]Department of Climate Change, Indian Institute of Technology Hyderabad, Kandi

Key Points:

- Southern (Northern) hemispheric eruptions extend (shorten) the Indian summer monsoon by several weeks in the year following the eruption.
- Volcanically forced changes in the Indian Summer Monsoon rainfall are driven by variations in the length of the monsoon season, rather than by changes in monsoon circulation strength.
- The forced shifts in the duration and onset of the monsoon are consistent with changes to the ITCZ and low-level jet instigated by the eruption.

This is a non-peer-reviewed preprint submitted to EarthArXiv.

The manuscript has been submitted to Geophysical Research Letters.

Corresponding author: Shreyas Iyer, `shreyas.iyer@mpimet.mpg.de`

Abstract

Large volcanic eruptions are a source of climate variability, affecting the seasonal mean precipitation of the Indian summer monsoon. However, the extent to which changes in seasonal precipitation can be attributed to variations in monsoon length vs. monsoon intensity has remained unclear. Using large ensemble simulations of idealised volcanic eruptions at varying latitudes, we find that the monsoon onset and withdrawal change by a few weeks compared to an unforced case. Southern (Northern) hemispheric eruptions extend (shorten) the Indian summer monsoon in the year following the eruption. We show that these changes in the length of the monsoon season are more important in controlling the response of total monsoon rainfall to eruptions than changes to the intensity of rainfall. We explain our results using the low-level jet and Inter-tropical Convergence Zone (ITCZ) frameworks, which have been used to explain the internal variability of the monsoon onset.

Plain Language Summary

Volcanic eruptions affect the summer monsoon rainfall in tropical regions, depending on their location. A majority of the water resources in the tropics are dependent on the monsoons. While the effects of volcanic eruptions on the monsoon season as a whole are well understood, changes to monsoon onset and withdrawal have remained unclear. Using large ensemble simulations of an Earth System Model, we find that volcanic eruptions change the onset and withdrawal of the Indian monsoon by a few weeks. The monsoon duration is extended following Southern hemispheric eruptions, but shortened following Northern hemispheric eruptions. We show that, contrary to the prevailing expectation, these changes in the length of the monsoon season have a stronger effect on the total rainfall in the monsoon season than changes to the intensity of rainfall. We explain these changes using two established frameworks for understanding the monsoon: first, via shifts in the Inter-tropical Convergence Zone, and second, through changes in moisture advection via the low-level jet.

1 Introduction

Large volcanic eruptions are an important source of short-term climate variability. The injection of sulphate aerosols into the stratosphere reduces incident shortwave radiation, causing surface cooling, and affecting the hydrological cycle (e.g., Robock, 2000; Timmreck, 2012; Simpson et al., 2019). Global precipitation decreases for 2-3 years following an eruption, with the largest reduction in tropical regions (Robock & Liu, 1994; Broccoli et al., 2003). However, the regional precipitation response is sensitive to both the magnitude and location of the eruption. In particular, this is true for monsoon rainfall, which can either be increased or decreased by volcanic eruptions depending on the eruption latitude (Liu et al., 2016; Zhuo et al., 2021).

One third of the global precipitation falls within the Intertropical Convergence Zone (ITCZ), a narrow band of intense rainfall in the tropics (Kang et al., 2018). Hence, small shifts in the ITCZ can have large impacts on regional precipitation. Extratropical volcanic eruptions preferentially cool the eruption hemisphere, shifting the ITCZ towards the opposite hemisphere due to shifts in energy balance (Kang et al., 2008; T. Schneider et al., 2014). This can promote or impede the seasonal migration of the ITCZ into the summer hemisphere, which affects the monsoon. An ITCZ shift towards the summer hemisphere is expected to increase summer monsoon rainfall, and vice versa. Consistently, Zhuo et al. (2021) and Liu et al. (2016) (using model studies), and Zuo et al. (2019) (using paleo proxies), show that monsoon precipitation increases after opposite-hemisphere eruptions and decreases after same-hemisphere extratropical eruptions. This reduction is correlated with the strength of the eruption, but significant decreases do not occur below a 10 Tg threshold of eruption strength (D'Agostino & Timmreck, 2022). Zhuo

et al. (2021) relate the volcanically-forced precipitation response to variations in the land-sea temperature contrasts, which change the intensity of the monsoon circulation.

While the seasonal-mean response of monsoon precipitation to volcanic eruptions is known, the effects of volcanic eruptions on the timing of the monsoon have remained unclear. In this study, we investigate how volcanic eruptions affect the onset, demise, and duration of the Indian Summer Monsoon (ISM), and demonstrate how changes in seasonal-mean precipitation arise from changes in monsoon duration.

The onset of the ISM is caused by increased surface wind convergence and upward moisture flux. This, in turn, is attributed to the strengthening of the Somali jet (or low-level jet, LLJ) (Findlater, 1969). This jet of westerly cross-equatorial winds is confined to a narrow region in the Arabian Sea and acts as a moisture source to the ISM. A stronger and more northward-displaced low-level jet in the pre-monsoon months has been associated with an earlier onset of the monsoon, which Chakraborty and Agrawal (2017) have explained using a West Asian heat low framework. They investigate interannual differences in onset dates over India and find that surface pressure anomalies over the region immediately west of India drive variations in the onset dates of the ISM. They suggest that the differential heating of land and sea over the region west of India (referred to as West Asia) creates a pressure gradient that strengthens the LLJ. A weakening of this pressure gradient is observed in years with a late onset and is accompanied by a weaker LLJ. In their study, surface pressure differences leading to shifted onset dates are seen months before the actual onset date. Hence, we expect the effect of volcanic eruptions on monsoon onset to be reflected in changes of the LLJ.

The variability of the timing of the ISM onset and withdrawal is of economic relevance, being critical to the region's agricultural output (Aijaz, 2013; Gadgil & Rupa Kumar, 2006). Variations in the duration and intensity of the ISM are also important to study, as they determine the ISM rainfall, which is responsible for the majority of the region's water resources (Noska & Misra, 2016). However, a majority of the studies on the ISM, including those that examine its response to eruptions, employ a fixed climatological period between May and September (Bombardi et al., 2020). Since the seasonal-mean monsoon response cannot determine changes to the onset and withdrawal, their responses to volcanic forcings remain unclear. Moreover, since the climatological rainy season doesn't coincide exactly with the actual onset and withdrawal of the monsoon, results can be influenced by the inclusion of dry season data (Xavier et al., 2007). Since studies that use a fixed monsoon period cannot attribute changes in ISM precipitation to changes in the monsoon duration, it remains unclear to what extent the volcanically forced changes in monsoon precipitation arise from changes in monsoon duration or monsoon intensity. Thus, using the global Earth System Model MPI-ESM, we investigate the following:

1. How do the ISM's life cycle characteristics (onset, demise and length) respond to volcanic eruptions?
2. How can these responses be explained within the ITCZ and LLJ frameworks of the monsoon?
3. What role does the monsoon season length play in determining the sensitivity of monsoon precipitation to volcanic eruptions?

2 Data and Methods

2.1 Data

The internal variability of the ISM makes it challenging to determine the impact of a single volcanic eruption. Only a few large eruptions exist in recorded history, so proxy reconstructions of historical data have been used to study the climate impact of volca-

noes (Crowley & Unterman, 2013). However, historical eruptions vary not only in eruption magnitude but also in location and season, which makes it challenging to understand the effects of any one of these factors. In contrast, large ensemble simulations with climate models can effectively separate internal variability from externally forced responses (Milinski et al., 2020). The effects of internal monsoon variability are averaged out with a sufficiently large ensemble. 100-member ensembles are large enough to detect the temperature changes following a volcanic eruption, both at a global (Milinski et al., 2020) and a regional scale (Pausata et al., 2020). We use a large ensemble of simulations of idealized volcanic eruptions with the Max Planck Institute Earth System Model, version 1.1-LR (MPI-ESM) (Giorgetta et al., 2013).

In MPI-ESM, the atmospheric general circulation model ECHAM6.3, with a horizontal resolution of 200km and 47 vertical levels up to 0.01 hPa (Stevens et al., 2013), including the land model JSBACH (Reick et al., 2021), is coupled with the ocean sea-ice model MPIOM, with a nominal horizontal resolution of 1.5° and 64 vertical levels (Jungclaus et al., 2013). The MPI-ESM has been used successfully to determine the climate response to volcanic eruptions (e.g. (D'Agostino & Timmreck, 2022; Azoulay et al., 2021; Zhuo et al., 2021)). It has shown agreement with other low-resolution CMIP6 models in intermodal comparison studies regarding global surface climate responses (Zanchettin et al., 2022). MPI-ESM simulations of the Pinatubo eruption also show agreement with observed data (Toohey et al., 2016).

We use and extend MPI-ESM's Easy Volcanic Aerosol Ensemble (EVA-Ens) (Azoulay et al., 2021), which simulates the effects of volcanic eruptions on the global climate by replacing the forcing fields for the June 1991 Pinatubo eruptions with idealised forcing fields. These fields are generated using the Easy Volcanic Aerosol (EVA) forcing generator (Toohey et al., 2016). The EVA generator calculates monthly-mean aerosol forcing input files as fields of single scattering albedo (SSA), wavelength-dependent aerosol extinction (EXT) and the asymmetry factor (ASY) as a function of volcanic sulphur emission, season, and location.

The EVA-Ens, containing tropical eruptions of varying strengths, is extended to include simulations of extratropical eruptions in the Northern and Southern hemispheres. We simulate 100 ensemble members for each eruption hemisphere from January 1991 to December 1995, with 6-hourly output. The volcanic eruptions occur in June 1991, corresponding to a strength of 40 Tg of sulphur, compared to an estimated 10 Tg of stratospheric sulphur emissions injected by the Mt. Pinatubo eruption (Timmreck, 2018). In addition to the three forced experiments, with tropical (**TR**), Northern hemispheric (**NH**) and Southern hemispheric (**SH**) eruptions, an unforced 100-member ensemble simulation is used as a control (**CTL**). Supplementary Figure S1 shows the distribution and movement of aerosols in the three forced experiments.

2.2 Definition of Monsoons

In this study, we define monsoon onset using spatially averaged precipitation data over land in the central Indian region: $70 - 85\,^{\circ}$E, $15 - 25\,^{\circ}$N. This region is a good representation of rainfall over the entire Indian Summer Monsoon region (Chakraborty & Agrawal, 2017; Noska & Misra, 2016). Following the methodology of Noska and Misra (2016), we compute the region-mean annual-mean rainfall climatology as an average over the 100 unforced ensemble members. For each ensemble member, the precipitation anomaly is found by subtracting the daily rainfall from the annual mean climatology. This anomaly is summated over a calendar year to find the cumulative anomaly. The day that corresponds to the minimum of the cumulative anomaly is one day prior to the monsoon onset. Similarly, the maximum of the cumulative anomaly is one day prior to the withdrawal of the monsoon. Monsoon onset, withdrawal, and length are determined for each ensemble member in each experiment for four post-eruption years (1992-1995).

2.3 Moisture Flux

Monsoon onset follows the strengthening of the LLJ due to increased convergence of moisture over the Indian subcontinent. The moisture flux $F_q(p)$ at a given pressure level p is:

$$F_q(p) = \rho(p)\, q(p)\mathbf{v}(p) \tag{1}$$

Where $\rho(p)$, $q(p)$, and $\mathbf{v}(p)$ are the density, specific humidity and horizontal velocity vector at pressure level p. From this, we find the column-integrated moisture flux:

$$F_q = \frac{1}{g}\int_{p_s}^{p_t} (q)\mathbf{v}\, dp \tag{2}$$

The moisture flux convergence (MFC) over central India is then calculated using the divergence theorem, which is the line integral of moisture flux over its boundary.

$$\text{MFC} = \sum_{70^\circ\text{E}}^{85^\circ\text{E}} F_q\Big|_{15^\circ\text{N}} - F_q\Big|_{25^\circ\text{N}} + \sum_{15^\circ\text{N}}^{25^\circ\text{N}} F_q\Big|_{70^\circ\text{E}} - F_q\Big|_{85^\circ\text{E}} \tag{3}$$

2.4 Determining the Latitude of the ITCZ

The position of the regional ITCZ at a given time over the Indian monsoon region is calculated as the meridional centroid of precipitation over the box 70−85 ° E, 30 ° N - 30 ° S. The centroid latitude of the precipitation is averaged over all ensemble members to obtain the latitude of the ITCZ.

3 Results

3.1 Variations in Monsoon Characteristics

Figure 1. (a) shows the variations in monsoon onset date in the first year following an eruption. Compared to the control run **CTL**, both the **TR** and **NH** experiments show a delay in the median onset by 4 and 12 days, respectively. Meanwhile, a 7-day advancement in the median onset date is observed in the **SH** experiment. Similarly, Figure 1. (b) shows the variations in monsoon demise date in the first year following an eruption. The median demise in the **TR** and **NH** experiments is advanced by 8.5 and 19.5 days, respectively, compared to the **CTL** experiment. A delay of 2 days in the median demise is seen in the **SH** experiment.

In each of the volcanically forced experiments, the onset and demise dates are shifted in opposing directions, causing large shifts in the monsoon length, seen in Figure 1. Compared to the median **CTL** monsoon duration of 119.5 days, the median **NH** experiment monsoon is shorter by 33.5 days, while the median **SH** experiment monsoon is 23.5 days longer.

Shifts in the monsoon life cycle are consistent with the displacement of the ITCZ following volcanic eruptions. In Figure 1. d), the movement of the regional tropical rain band is compared across the four experiments. We find, relative to **CTL**, a Southward-shifted ITCZ in the **NH** experiment, and a Northward-shifted ITCZ in the **SH** experiment.

In the **NH** experiment, the South-shifted ITCZ delays the arrival of the ITCZ to the Indian subcontinent, causing a delay in onset. Similarly, it would speed up its departure from the subcontinent, causing an earlier withdrawal. In the **TR** experiment, the ITCZ is shifted southward as well, although by a lower magnitude compared to **NH**. This is in agreement with the relatively smaller shift in monsoon onset and withdrawal.

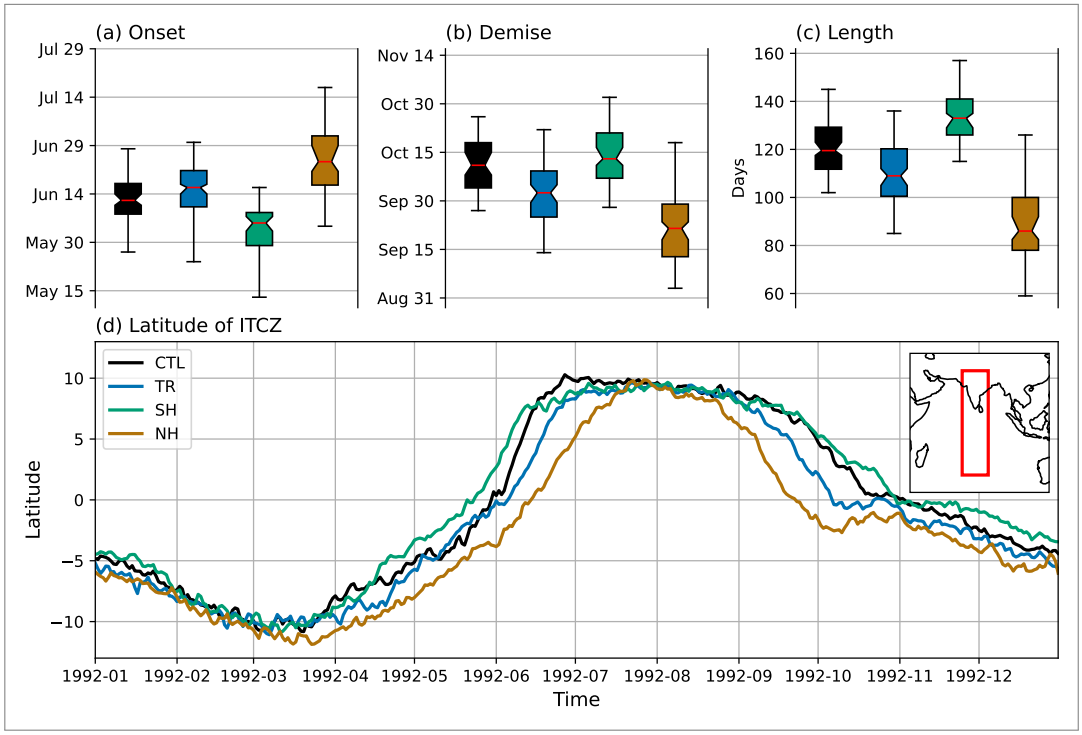

Figure 1. Variation of monsoon (a) onset, (b) demise, and (c) length for the first post-eruption year (1992). The boxes show the interquartile range of ensemble members, while the whiskers contain 95% of values around the median (red line). Notches indicate the 95% confidence interval around the median generated by bootstrapping 50 of the 100 members with 10,000 resamples. (d) Movement of the ensemble-mean latitude of the tropical (30°S–30°N) precipitation centroid in the longitude band 70–85°E (red rectangle in inset).

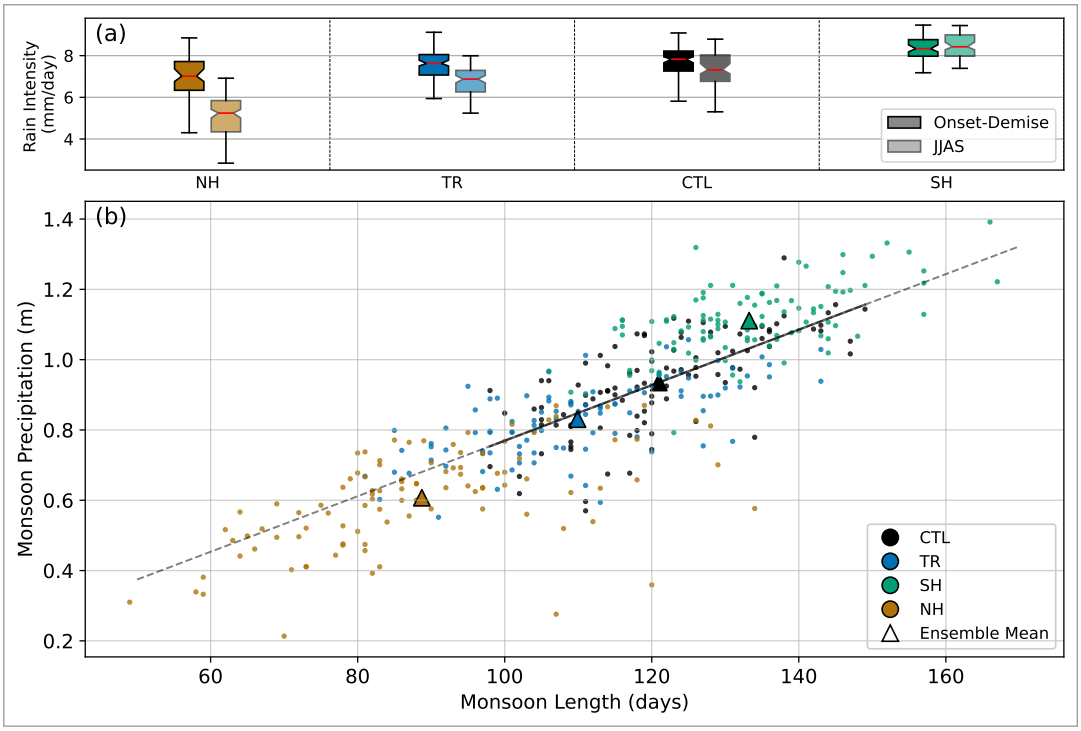

Figure 2. (a) Box plot comparing the usage of a fixed (JJAS) and variable (defined by the onset and demise) monsoon duration on the mean monsoon intensity for the four experiments. Boxes show the interquartile range of ensemble members, and whiskers contain 95% of values around the median (red line). Notches indicate the 95% confidence interval around the median generated by bootstrapping 50 of the 100 members with 10,000 resamples. The (b) Scatter plot of the monsoon season precipitation and length in the year 1992 for the four experiments. The linear regression (r = 0.69) of precipitation and length for the CTL experiment is shown in the solid black curve and is extended to the width of the graph with the dashed line.

Conversely, in the **SH** experiment, the displacement of the ITCZ to the North results in an earlier onset and later withdrawal.

3.2 Monsoon Duration Controls Seasonal Precipitation

Having demonstrated that the monsoon duration is strongly influenced by extra-tropical volcanic eruptions, we now investigate how this affects the seasonal rainfall. The large variations in monsoon duration highlight the limitation of quantifying monsoon-season averages over a fixed period. When using a fixed duration of the monsoon, JJAS (Jun-Jul-Aug-Sep), the season-mean precipitation intensities in the forced experiments show a large variation compared to **CTL** (Figure 2 (a)). The average JJAS intensity in the **NH** experiment is 2 mm/day lower than in **CTL**, while it is 1 mm/day higher in the **SH** experiment. However, the JJAS intensity is not an adequate representation of the monsoon intensity when there are large changes in the climatological rainy season, as caused by volcanic eruptions. By using a variable length of the monsoon, we exclude data from the dry season, enabling an accurate assessment of the true monsoon intensity.

Defining the monsoon season as the period between onset and demise results in smaller variations of mean monsoon intensity in the forced experiments. The average onset-to-

demise intensity in the **NH** experiment is 0.8 mm/day lower than in **CTL**, while it is 0.5 mm/day higher in the **SH** experiment. An analysis using a fixed monsoon climatology neglects the volcanic impact on the monsoon duration. It leads to the spurious conclusion that the variations in the total monsoon rainfall arise from changes in its intensity. Using a variable monsoon duration allows us to determine the extent to which changes in rainfall are influenced by changes in duration, rather than intensity.

Figure 2 (b) shows the relation between the total monsoon precipitation and the monsoon duration. The regression (r = 0.69) of the **CTL** precipitation and length indicates that the variation of monsoon duration explains the majority of changes in monsoon precipitation. Based on the linear relationship, we would expect a 90-day monsoon (the length of the ensemble-mean **NH** monsoon) to see an integrated rainfall deficit of 300 mm, compared to the climatological 0.95 m during a 120-day monsoon. As a result, the 350 mm deficit of rainfall seen during the **NH** ensemble-mean monsoon can largely be explained by a shorter monsoon period, while only 50 mm is due to changes in the monsoon intensity. This shows that the dominant factor in altering the seasonal precipitation response of the ISM following a volcanic eruption is the length of the monsoon, contrary to the current understanding that the volcanically-forced precipitation response mainly arises from changing rainfall intensity due to changing land-sea contrasts (Zhuo et al., 2021).

3.3 Variations in the Strength of the Low-Level Jet

Although the ITCZ framework provides a qualitatively consistent picture, the rainfall over India is not zonally symmetric, nor is it affected solely by inter-hemispheric temperature contrasts. In the following, we analyse the effects of zonally asymmetric cooling and changes in pressure gradients and moisture fluxes on the monsoon.

In Figures 3 (b), (c), in the **NH** and **TR** experiments, respectively, the sea level pressure (SLP) directly west of the subcontinent (in the Arabian Sea) in the premonsoon month of May is anomalously high. Whereas, in the **SH** experiment in 3 (d), we find an anomalous pressure low. This is consistent with the observed real-world internal variability of the monsoon, where an anomalously high 'West Asian' pressure is associated with a delayed monsoon onset (Chakraborty & Agrawal, 2017). The delayed onset is correlated with a weakened LLJ, as seen in the Arabian Sea and Indian Ocean, characterised by anomalous Easterly (Westerly) winds North (South) of the equator and an anomalous high pressure over this region. However, contrary to our expectation, an anomalously strong jet over India is not seen in the **SH** experiment, despite both an anomalously low SLP and early onset (Figure 3 (d)).

To explain this apparent inconsistency, we analyse the moisture flux into the ISM region. While the LLJ strength in the Arabian Sea controls the moisture influx into the subcontinent, the onset of the ISM occurs due to the convergence of this moisture flux, and is also dependent on the outflux of moisture. Figure 3 (a) shows that large moisture convergence occurs in the days before onset. Despite the weak LLJ in May, there is a sudden increase in moisture convergence over India in the **SH** experiment, leading to an earlier onset. Supplementary Figure S2 shows the moisture fluxes at the boundary of the central Indian box for each experiment.

4 Discussion and Conclusion

Previous studies of the monsoon region have investigated how volcanic forcings affect the seasonal average rainfall of the monsoon region (e.g., D. P. Schneider et al. (2009); Zuo et al. (2019); D'Agostino and Timmreck (2022); Liu et al. (2016)). They attribute changes in the seasonal mean rainfall to a change in the strength of the monsoon circulation driven by differential land-sea cooling. However, observational data have shown

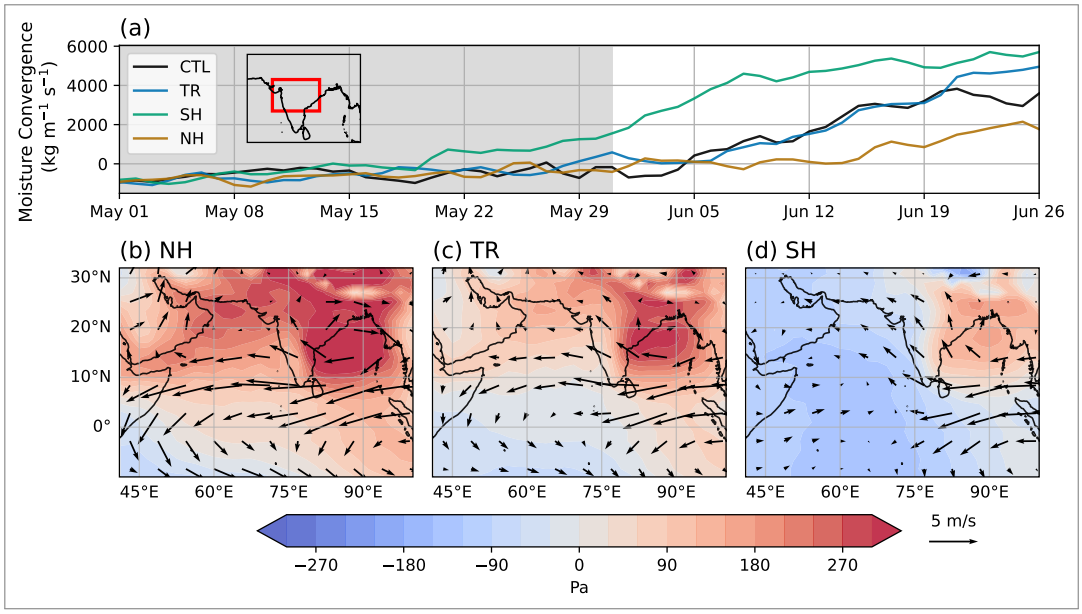

Figure 3. (a) The ensemble-mean vertically integrated moisture flux into central India during the 1992 boreal summer (red rectangle in the inset: 70–85°E, 15–25°N) for all four experiments. The grey box shows the month of May, over which time the composite (b) **NH**, (c) **TR**, and (d) **SH** anomalous ensemble-mean sea level pressure in 1992, with respect to the ensemble mean **CTL**, is calculated. The black arrows denote the ensemble-mean 850hPa horizontal wind velocity vector anomalies for the same.

that the total monsoon rainfall is correlated with the seasonal length (Noska & Misra, 2016). Our results show that using an average rainfall intensity over a fixed monsoon season fails to account for changes in the duration of the monsoon season and its impact on the total monsoon rainfall.

In our study, we find changes in the life cycle of the ISM for several years after volcanic eruptions, comparable to the lifetime of stratospheric sulphur aerosols, as shown in Supplementary Figure S3. However, certain geoengineering scenarios, such as stratospheric aerosol intervention (SAI), are designed to exert longer-term climatic effects. SAI studies (e.g., Simpson et al. (2019)) show a reduction in the JJA rainfall over India. This reduction in rainfall is likely also driven primarily by a shorter monsoon length. Shifts in the ISM's timing and duration should be considered, since crop sowing is dependent on the timing of the ISM (Nageswararao et al., 2024). Although certain SAI strategies are likely to strengthen certain regional monsoons (e.g., SAI confined to the Southern Hemisphere would strengthen ISM), they would weaken other regional monsoons.

The life cycle of other regional monsoons is expected to behave similarly to the ISM, when forced by volcanic eruptions. In the context of the ITCZ framework, we would expect an eruption in the same (opposite) hemisphere to shorten (lengthen) the monsoon season. Since our methodology does not employ rigid thresholds in defining monsoon onset and demise, it can be applied, with a few modifications, to identify and compare the responses of all regional monsoons to volcanic forcings in our model.

The impact of volcanic eruptions on internal modes of variability, such as the El Niño-Southern Oscillation (ENSO), has been studied (e.g., Stevenson et al. (2016); Pausata et al. (2020); Fang et al. (2025)). Fang et al. (2025) note the presence of a strong El Niño (weak La Niña) in the few years following a Northern (Southern) hemisphere eruption.

ENSO significantly forces the ISM's precipitation and onset, with shorter and weaker (longer and stronger) ISMs in El Nino (La Nina) years. (e.g., Goswami and Xavier (2005); Fan et al. (2017); Chakraborty and Singhai (2021)) However, monsoon anomalies tend to be stronger in El Niño years. Thus, there are asymmetries in both the monsoon response to the ENSO phase and the ENSO response to the location of volcanic eruption. These asymmetries reinforce each other, leading to a stronger monsoon response to Northern Hemisphere eruptions. These reinforcing asymmetries could provide an explanation as to why we find stronger anomalies in ISM rainfall in the **NH** experiment compared to the **SH** experiment.

However, the MPI-ESM was run in a coarse-resolution configuration, with a horizontal resolution of 200 km, due to which the influence of orography, and orographic rainfall is greatly reduced, which is important to represent the monsoon (Chakraborty et al., 2006). Additionally, convection in the MPI-ESM is parametrised, limiting its ability to represent changes in convective rainfall due to volcanic forcing. Furthermore, the experiments prescribe volcanic forcings with a strength of 40 TgS compared to 5–10 TgS from Pinatubo (Timmreck, 2018). Such large eruptions are exceedingly rare. Smaller eruptions would have a smaller climate impact, but the impacts are expected to scale roughly linearly with the sulphur injection (Timmreck et al., 2024).

In this study, we find, using large ensemble simulations of the MPI-ESM, that large volcanic eruptions shift the onset, withdrawal and length of the Indian summer monsoon for a few years. Northern hemispheric and tropical eruptions delay the onset and advance the demise of the ISM, leading to a shorter monsoon season. Conversely, Southern hemispheric eruptions advance the onset and delay the demise of the ISM, lengthening its duration. We explain this within the ITCZ framework of the monsoons, where ITCZ shifts towards the monsoon hemisphere causing an earlier onset and delayed demise. The framework of monsoon onset driven by the strengthening of the LLJ successfully explains the delayed onset in **NH** and **TR**, but cannot fully explain the earlier onset in **SH** in a comprehensive way. We find that in **SH**, despite no significant increases in LLJ strength, early monsoon onset occurs due to increased moisture convergence. We show that the shift in Indian summer monsoon rainfall, caused by volcanic forcings, is driven predominantly by changes in the duration of the monsoon season and not, as previously thought, by changes in the intensity of the monsoon precipitation. Future studies should take into account the varying monsoon season length in order to clearly distinguish between changes to monsoon intensity versus length.

Open Research Section

The data and code supporting the conclusions of this study are available at Edmond (Iyer et al., 2026) at the link: https://doi.org/10.17617/3.GYBFO1

Conflict of Interest declaration

The authors declare there are no conflicts of interest for this manuscript.

Acknowledgments

Shreyas Iyer would like to thank the IISER-Max Planck Society partner program, which enabled his research stay at the Max Planck Institute for Meteorology in 2024/2025, and funding from the KVPY-INSPIRE fellowship. Claudia Timmreck acknowledges funding by the German National funding agency (DFG) within the research unit FOR 2820 (VolImpact, Project Number: 398006378). MG acknowledges funding by the joint Max-Planck/Weizmann Postdoctoral Program. Computations and analysis were performed

on the computer of the Deutsches Klima Rechenzentrum (DKRZ) using resources granted by its Scientific Steering Committee (WLA) under project ID bb1093.

References

Aijaz, R. (2013, May). *Monsoon Variability and Agricultural Drought Management in India.* https://www.orfonline.org/research/monsoon-variability-and-agricultural-drought-management-in-india.

Azoulay, A., Schmidt, H., & Timmreck, C. (2021). The Arctic Polar Vortex Response to Volcanic Forcing of Different Strengths. *Journal of Geophysical Research: Atmospheres*, *126*(11), e2020JD034450. doi: 10.1029/2020JD034450

Bombardi, R. J., Moron, V., & Goodnight, J. S. (2020, February). Detection, variability, and predictability of monsoon onset and withdrawal dates: A review. *International Journal of Climatology*, *40*(2), 641–667. doi: 10.1002/joc.6264

Broccoli, A. J., Dixon, K. W., Delworth, T. L., Knutson, T. R., Stouffer, R. J., & Zeng, F. (2003). Twentieth-century temperature and precipitation trends in ensemble climate simulations including natural and anthropogenic forcing. *Journal of Geophysical Research: Atmospheres*, *108*(D24). doi: 10.1029/2003JD003812

Chakraborty, A., & Agrawal, S. (2017, July). Role of west Asian surface pressure in summer monsoon onset over central India. *Environmental Research Letters*, *12*(7), 074002. doi: 10.1088/1748-9326/aa76ca

Chakraborty, A., Nanjundiah, R. S., & Srinivasan, J. (2006, September). Theoretical aspects of the onset of Indian summer monsoon from perturbed orography simulations in a GCM. *Annales Geophysicae*, *24*(8), 2075–2089. doi: 10.5194/angeo-24-2075-2006

Chakraborty, A., & Singhai, P. (2021, November). Asymmetric response of the Indian summer monsoon to positive and negative phases of major tropical climate patterns. *Scientific Reports*, *11*(1), 22561. doi: 10.1038/s41598-021-01758-6

Crowley, T. J., & Unterman, M. B. (2013, May). Technical details concerning development of a 1200 yr proxy index for global volcanism. *Earth System Science Data*, *5*(1), 187–197. doi: 10.5194/essd-5-187-2013

D'Agostino, R., & Timmreck, C. (2022, May). Sensitivity of regional monsoons to idealised equatorial volcanic eruption of different sulfur emission strengths. *Environmental Research Letters*, *17*(5), 054001. doi: 10.1088/1748-9326/ac62af

Fan, F., Dong, X., Fang, X., Xue, F., Zheng, F., & Zhu, J. (2017). Revisiting the relationship between the South Asian summer monsoon drought and El Niño warming pattern. *Atmospheric Science Letters*, *18*(4), 175–182. doi: 10.1002/asl.740

Fang, S.-W., Pausata, F. S. R., D'Agostino, R., Khodri, M., Zanchettin, D., & Timmreck, C. (2025, November). Seasonal ITCZ Control on ENSO Responses to Extratropical Volcanic Forcing. *Journal of Climate*, *38*(21), 6061–6079. doi: 10.1175/JCLI-D-24-0554.1

Findlater, J. (1969). A major low-level air current near the Indian Ocean during the northern summer. *Quarterly Journal of the Royal Meteorological Society*, *95*(404), 362–380. doi: 10.1002/qj.49709540409

Gadgil, S., & Rupa Kumar, K. (2006). The Asian monsoon — agriculture and economy. In B. Wang (Ed.), *The Asian Monsoon* (pp. 651–683). Berlin, Heidelberg: Springer. doi: 10.1007/3-540-37722-0_18

Giorgetta, M. A., Jungclaus, J., Reick, C. H., Legutke, S., Bader, J., Böttinger, M., ... Stevens, B. (2013). Climate and carbon cycle changes from 1850 to 2100 in MPI-ESM simulations for the Coupled Model Intercomparison Project phase 5. *Journal of Advances in Modeling Earth Systems*, *5*(3), 572–597. doi: 10.1002/jame.20038

Goswami, B. N., & Xavier, P. K. (2005). ENSO control on the south Asian monsoon through the length of the rainy season. *Geophysical Research Letters*, *32*(18). doi: 10.1029/2005GL023216

Iyer, S., Günther, M., Jalihal, C., & Timmreck, C. (2026). *The Response of Onset and Withdrawal of the Indian Summer Monsoon to Volcanic Aerosols.* Edmond. Retrieved from `https://doi.org/10.17617/3.GYBFO1` doi: 10.17617/3.GYBFO1

Jungclaus, J. H., Fischer, N., Haak, H., Lohmann, K., Marotzke, J., Matei, D., ... von Storch, J. S. (2013). Characteristics of the ocean simulations in the Max Planck Institute Ocean Model (MPIOM) the ocean component of the MPI-Earth system model. *Journal of Advances in Modeling Earth Systems*, *5*(2), 422–446. doi: 10.1002/jame.20023

Kang, S. M., Held, I. M., Frierson, D. M. W., & Zhao, M. (2008, July). The response of the ITCZ to extratropical thermal forcing: Idealized slab-ocean experiments with a GCM. *Journal of Climate*, *21*(14), 3521–3532. doi: 10.1175/2007JCLI2146.1

Kang, S. M., Shin, Y., & Xie, S.-P. (2018, January). Extratropical forcing and tropical rainfall distribution: Energetics framework and ocean Ekman advection. *npj Climate and Atmospheric Science*, *1*(1), 20172. doi: 10.1038/s41612-017-0004-6

Liu, F., Chai, J., Wang, B., Liu, J., Zhang, X., & Wang, Z. (2016, April). Global monsoon precipitation responses to large volcanic eruptions. *Scientific Reports*, *6*(1), 24331. doi: 10.1038/srep24331

Milinski, S., Maher, N., & Olonscheck, D. (2020, October). How large does a large ensemble need to be? *Earth System Dynamics*, *11*(4), 885–901. doi: 10.5194/esd-11-885-2020

Nageswararao, M. M., Joseph, S., Mandal, R., Tallapragada, V., Akhter, J., Dey, A., ... Sahai, A. K. (2024, November). The role of antecedent southwest summer monsoon rainfall on the occurrence of premonsoon heat waves over India in the present global warming era. *Discover Environment*, *2*(1), 127. doi: 10.1007/s44274-024-00166-7

Noska, R., & Misra, V. (2016, May). Characterizing the onset and demise of the Indian summer monsoon. *Geophysical Research Letters*, *43*(9), 4547–4554. doi: 10.1002/2016GL068409

Pausata, F. S. R., Zanchettin, D., Karamperidou, C., Caballero, R., & Battisti, D. S. (2020, June). ITCZ shift and extratropical teleconnections drive ENSO response to volcanic eruptions. *Science Advances*, *6*(23), eaaz5006. doi: 10.1126/sciadv.aaz5006

Reick, C. H., Gayler, V., Goll, D., Hagemann, S., Heidkamp, M., Nabel, J. E. M. S., ... Wilkenskjeld, S. (2021). *JSBACH 3 - The land component of the MPI Earth System Model: documentation of version 3.2* (Vol. 240). Hamburg: MPI für Meteorologie. doi: 10.17617/2.3279802

Robock, A. (2000, May). Volcanic eruptions and climate. *Reviews of Geophysics*, *38*(2), 191–219. doi: 10.1029/1998RG000054

Robock, A., & Liu, Y. (1994, January). The Volcanic Signal in Goddard Institute for Space Studies Three-Dimensional Model Simulations. *Journal of Climate*, *7*(1), 44–55. doi: 10.1175/1520-0442(1994)007⟨0044:TVSIGI⟩2.0.CO;2

Schneider, D. P., Ammann, C. M., Otto-Bliesner, B. L., & Kaufman, D. S. (2009). Climate response to large, high-latitude and low-latitude volcanic eruptions in the Community Climate System Model. *Journal of Geophysical Research: Atmospheres*, *114*(D15). doi: 10.1029/2008JD011222

Schneider, T., Bischoff, T., & Haug, G. H. (2014, September). Migrations and dynamics of the intertropical convergence zone. *Nature*, *513*(7516), 45–53. doi: 10.1038/nature13636

Simpson, I. R., Tilmes, S., Richter, J. H., Kravitz, B., MacMartin, D. G., Mills,

M. J., ... Pendergrass, A. G. (2019). The Regional Hydroclimate Response to Stratospheric Sulfate Geoengineering and the Role of Stratospheric Heating. *Journal of Geophysical Research: Atmospheres*, *124*(23), 12587–12616. doi: 10.1029/2019JD031093

Stevens, B., Giorgetta, M., Esch, M., Mauritsen, T., Crueger, T., Rast, S., ... Roeckner, E. (2013). Atmospheric component of the MPI-M Earth System Model: ECHAM6. *Journal of Advances in Modeling Earth Systems*, *5*(2), 146–172. doi: 10.1002/jame.20015

Stevenson, S., Otto-Bliesner, B., Fasullo, J., & Brady, E. (2016, April). "El Niño Like" Hydroclimate Responses to Last Millennium Volcanic Eruptions. *Journal of Climate*, *29*(8), 2907–2921. doi: 10.1175/JCLI-D-15-0239.1

Timmreck, C. (2012). Modeling the climatic effects of large explosive volcanic eruptions. *WIREs Climate Change*, *3*(6), 545–564. doi: 10.1002/wcc.192

Timmreck, C. (2018). *Climatic effects of large volcanic eruptions* (habilitation, Max-Planck-Institut für Meteorologie, Hamburg). doi: 10.17617/2.2566000

Timmreck, C., Olonscheck, D., Ballinger, A. P., D'Agostino, R., Fang, S.-W., Schurer, A. P., & Hegerl, G. C. (2024, March). Linearity of the Climate Response to Increasingly Strong Tropical Volcanic Eruptions in a Large Ensemble Framework. *Journal of Climate*, *37*(8), 2455–2470. doi: 10.1175/JCLI-D-23-0408.1

Toohey, M., Stevens, B., Schmidt, H., & Timmreck, C. (2016, November). Easy Volcanic Aerosol (EVA v1.0): An idealized forcing generator for climate simulations. *Geoscientific Model Development*, *9*(11), 4049–4070. doi: 10.5194/gmd-9-4049-2016

Xavier, P. K., Marzin, C., & Goswami, B. N. (2007). An objective definition of the Indian summer monsoon season and a new perspective on the ENSO–monsoon relationship. *Quarterly Journal of the Royal Meteorological Society*, *133*(624), 749–764. doi: 10.1002/qj.45

Zanchettin, D., Timmreck, C., Khodri, M., Schmidt, A., Toohey, M., Abe, M., ... Weierbach, H. (2022, March). Effects of forcing differences and initial conditions on inter-model agreement in the VolMIP volc-pinatubo-full experiment. *Geoscientific Model Development*, *15*(5), 2265–2292. doi: 10.5194/gmd-15-2265-2022

Zhuo, Z., Kirchner, I., Pfahl, S., & Cubasch, U. (2021, September). Climate impact of volcanic eruptions: The sensitivity to eruption season and latitude in MPI-ESM ensemble experiments. *Atmospheric Chemistry and Physics*, *21*(17), 13425–13442. doi: 10.5194/acp-21-13425-2021

Zuo, M., Zhou, T., & Man, W. (2019, July). Hydroclimate Responses over Global Monsoon Regions Following Volcanic Eruptions at Different Latitudes. *Journal of Climate*, *32*(14), 4367–4385. doi: 10.1175/JCLI-D-18-0707.1

Supporting Information for "The Response of Onset and Withdrawal of the Indian Summer Monsoon to Volcanic Aerosols"

S. Iyer[1,2], M. Günther[1], C. Jalihal[1,3], and C. Timmreck[1]

[1]Max Planck Institute for Meteorology, Hamburg

[2]Indian Institute of Science Education and Research, Pune

[3]Department of Climate Change, Indian Institute of Technology Hyderabad, Kandi

Contents of this file

1. Supplementary Figures S1 to S3

Introduction

The supporting information includes three supplementary figures that are referenced but not presented in the main text.

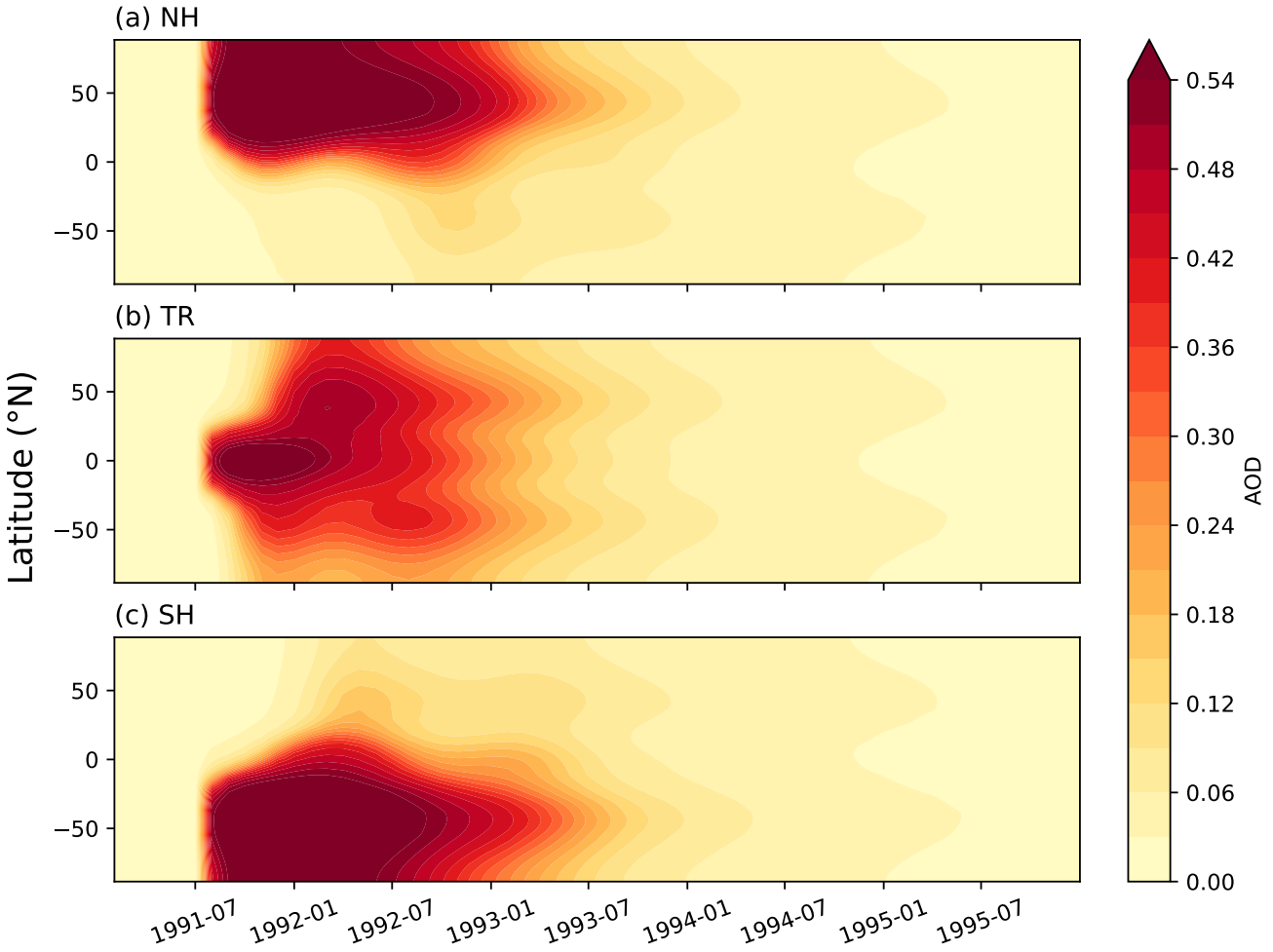

Figure S1. The time evolution of aerosol optical depth at 550 nm for (a) Northern Hemisphere, (b) Tropical and (c) Southern Hemisphere volcanic eruption of 40 Tg of Sulphur, corresponding to the experiments **NH**, **TR**, and **SH** respectively.

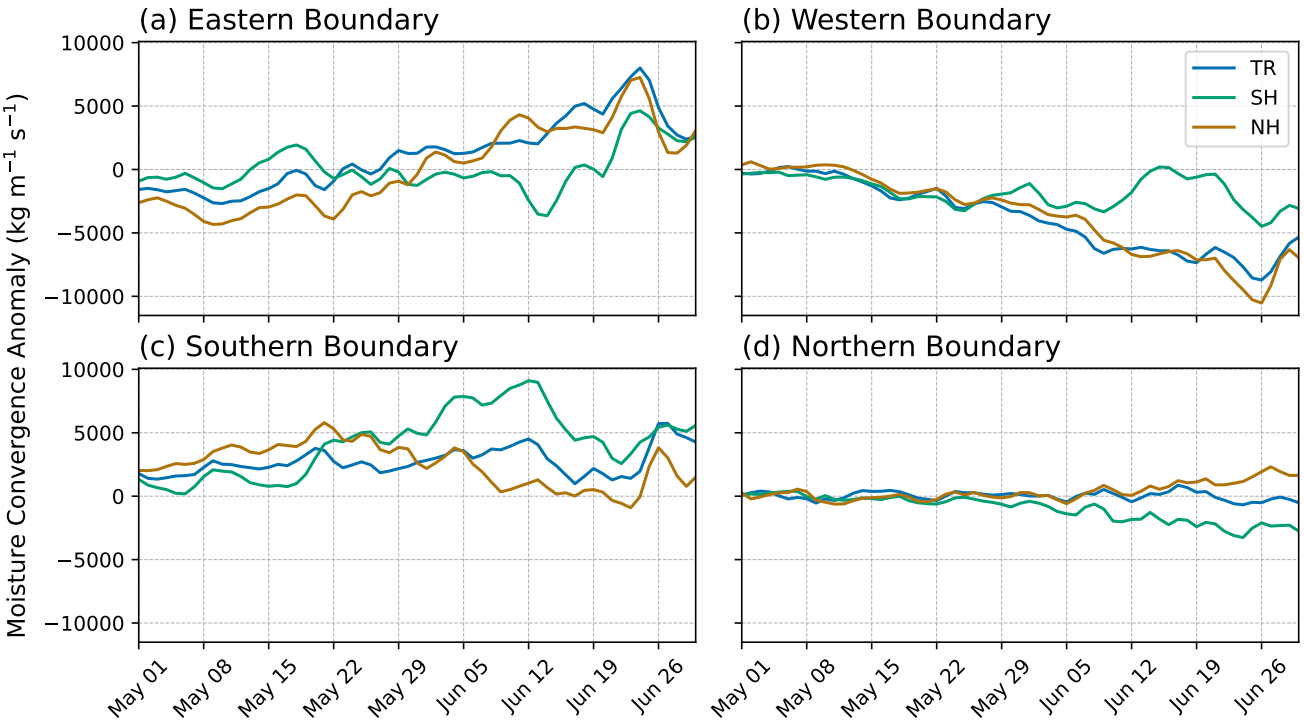

Figure S2. The anomalous moisture flux at the (a) Eastern, (b) Western, (c) Southern, and (d) Northern boundaries of the Central Indian region, with respect to **CTL** for the three forced experiments in the months of May and June 1992.

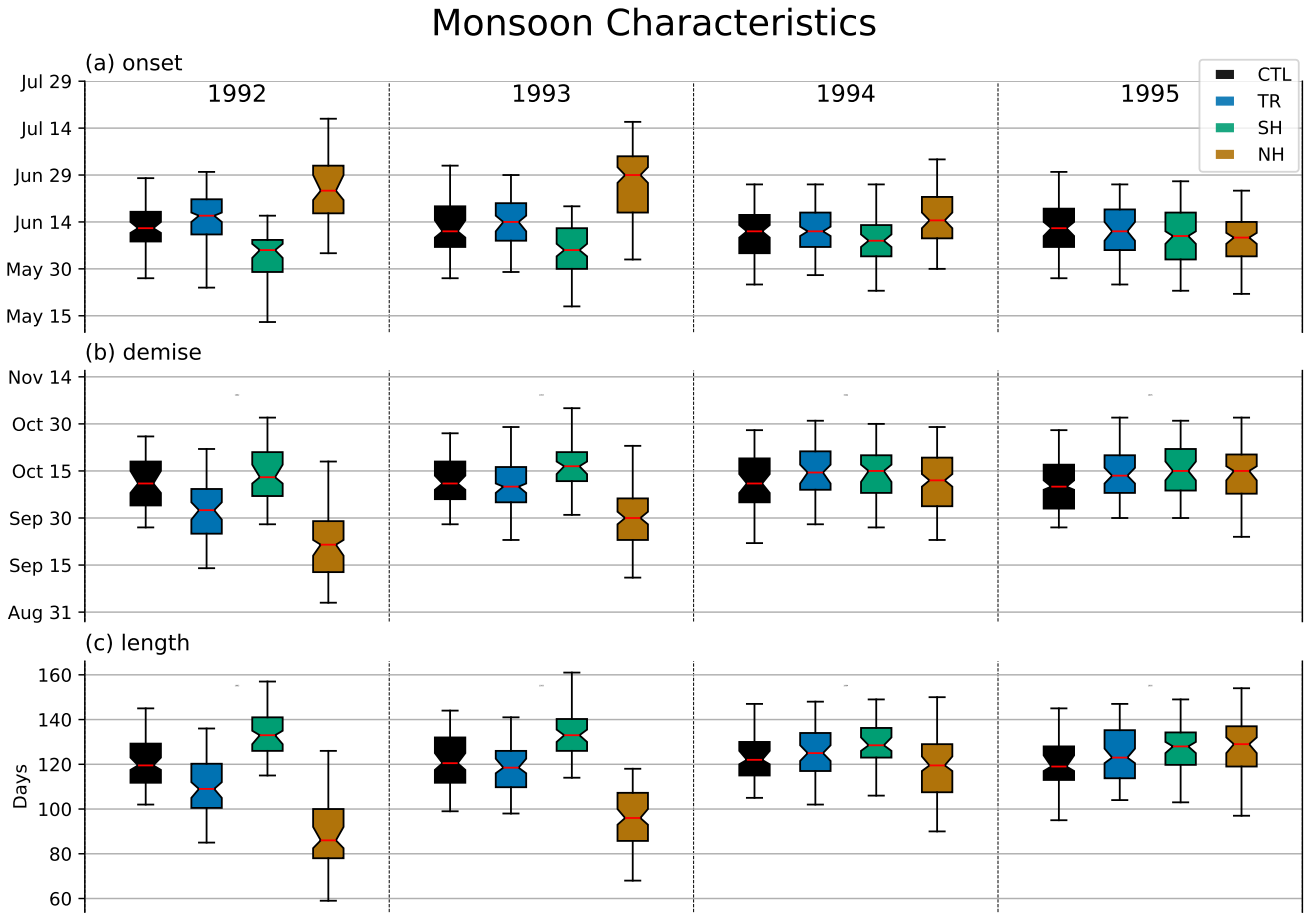

Figure S3. Monsoon (a) onset, (b) demise, and (c) length for the years 1992 to 1995. The boxes represent the interquartile range of ensemble members, while the whiskers encompass 95% of the values around the median (red line). Notches indicate the 95% confidence interval around the median generated by bootstrapping 50 of the 100 members with 10,000 resamples.